15th Triennial World Congress, Barcelona, Spain

ELECTRONIC CONTROL OF A MULTI-PHASE LIGHTING SYSTEM

Roberto Zanasi, * **Germano Sandoni** *

* *University of Modena and Reggio Emilia, DSI*
Via Vignolese 905, 41100 Modena, Italy,
Phone: +39 59 2056161, Fax: +39 59 2056126
E-mails: roberto.zanasi@unimo.it,
sandoni.germano@unimo.it

Abstract: In the paper, the dynamic model of a lighting system is taken into account and a simple control strategy for controlling the load voltages is presented. All the main components of the electronic system (supply, rectifier, capacitive filter, inverter, etc.) have been modelled in details by using the graphical modelling technique named Power-Oriented Graphs. A control strategy for minimizing the neutral current i_N is also presented. Simulation results show the effectiveness of the presented control strategies.

Keywords: Algorithms, Control system design, Models, System analysis, Light, Electronic systems.

1. INTRODUCTION

In the most of the actual lighting systems the load voltages are controlled by using an electro-mechanical driving system (see Fig. 1): the desired

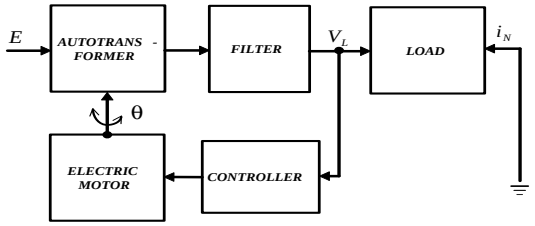

Fig. 1. Electro-mechanical control of the voltage.

load voltages $\mathbf{V}_L$ on the lamps are determined by the cursor position θ of the autotransformer. This electro-mechanical control system is slow, inaccurate in the transient and subject to mechanical wear. For solving these problems, in this paper a new electronic control system is presented and analyzed. All the main components of the lighting system have been modelled by using a graphical technique named Power-Oriented Graphs (POG), see (Zanasi, 1991) and (Zanasi, 1994). A control strategy for controlling the voltages on the lamps is also presented. The effectiveness of the control strategy is tested in simulation and then optimized trying to minimize the neutral current. The paper is organized as follows. The controlled system and the control requirements are described in Section 2. The POG dynamic model of the lighting system is presented in Section 3. A simple control strategy for controlling the voltages on the lamps and an algorithm for the minimization of the neutral current i_N are described in Section 4 together with simulation results that validate the proposed control strategies.

2. CONTROLLED SYSTEM

The electric scheme of the considered lighting system is shown in Fig. 2. It is composed of five blocks: three-phase power, graetz rectifier, capacitive filter, IGBT inverters and the loads. The three-phase 220 Vrms power supply provides a set

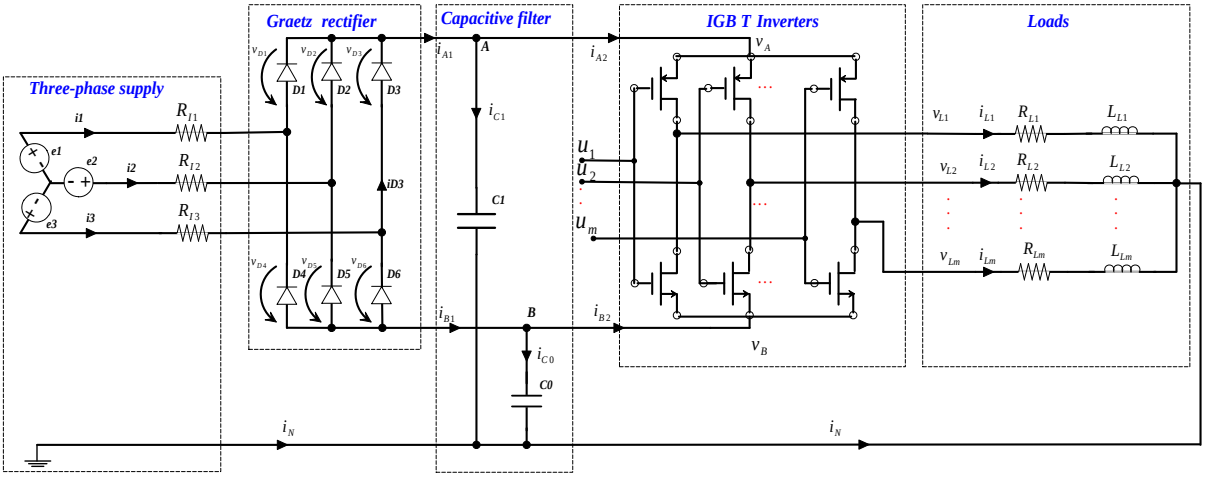

Fig. 2. Electric scheme used for controlling the output voltages $\mathbf{V}_L$ of the lighting system.

of three direct phase voltages: $\mathbf{E} = [e_1, e_2, e_3]^{\mathrm{T}}$. In this block, the supply internal resistances R_{Ii}, $i = \{1, 2, 3\}$ are also considered. The second block is a simple three-phase full wave diode rectifier that converts the AC three-phase voltages into a DC voltage. The third block is the capacitive filter whose purpose is to reduce the ripple on the voltages $v_A(t)$ and $v_B(t)$, see Fig. 2. The IGBT inverters are driven by the control vector $\mathbf{u}(t) = [u_1(t), u_2(t), \ldots, u_m(t)]^{\mathrm{T}}$. The loads are composed by lines of lamps connected in shunt. For each line of lamps a couple of IGBT is necessary. In Fig. 2 the case of m lines of lamps is shown. The number of lamps for each line is not determinabile, so the loads are usually not balanced.

2.1 Control requirements

The control vector $\mathbf{u}(t)$ has to be chosen to satisfy the following requirements:

(1) The load voltages $\mathbf{V}_L$ must be sinusoidal despite of the voltage ripple on the A and B points.
(2) The load voltages $\mathbf{V}_L$ should have an amplitude of 220 Vrms $\pm 2\%$, even in presence of a fluctuation of $\pm 10\%$ of the three-phase supply.
(3) The neutral current i_N should be minimized to optimize the energy dissipation.

3. DYNAMIC-MODEL OF THE LIGHTING SYSTEM

3.1 Power-Oriented Graphs: basic concepts

The main idea of this graphical technique is to use the "power interaction" between sub-systems as basic element for modelling. The "bond graph" technique (Paynter, 1961), (Karnopp, 1975) is based on the same idea, but uses a different graphical representation. By keeping "coupled" the variables which are "conjugate" with respect to power, these graphical techniques provide graphical dynamic models which, usually, are intuitive and easy to use. The "Power-Oriented Graphs" are "signal flow graphs" combined with a particular "modular" structure essentially based on the two blocks shown in Fig. 3. The basic characteristic of this structure is the direct correspondence between pairs of system variables and real power flows: the product of the two variables involved in each dashed line of the graph has the physical meaning of "power flowing through the section". The two basic blocks shown in Fig. 3 are named

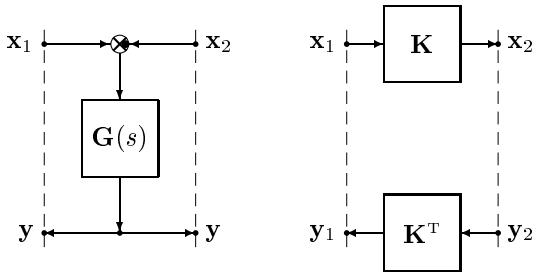

Fig. 3. Basic blocks: elaboration block (e.b.) and connection block (c.b.).

"elaboration block" (e.b.) and "connection block" (c.b.). The inner product $\langle \mathbf{x}, \mathbf{y} \rangle = \mathbf{x}^{\mathrm{T}}\mathbf{y}$ must have the physical meaning of a "power". The e.b. and the c.b. are suitable for representing both scalar and vectorial systems. While the elaboration block can store and dissipate energy (i.e. springs, masses and dampers), the connection block can only "transform" the energy, that is, transform the system variables from one type of energy-field to another (i.e. any type of gear reduction). For a more detailed description of the POG graphical technique, please refer to (Zanasi, 1991) and (Zanasi, 1994).

3.2 POG model of the lighting system

The multi-dimensional POG model of the electric scheme of Fig. 2, is shown in Fig. 4. Observe the

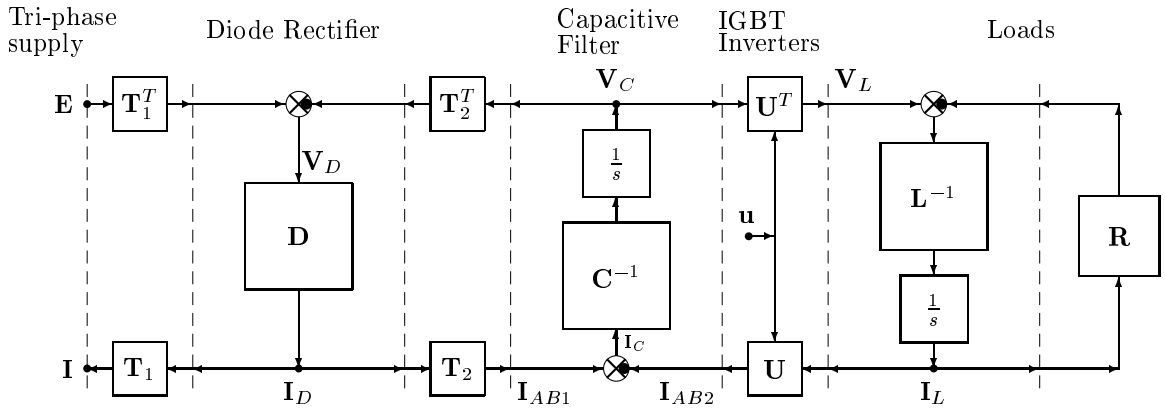

Fig. 4. POG dynamic model of the lighting system.

direct correspondence between the POG blocks and physical elements of the electric scheme. The variables which are present in the POG model are the following: $\mathbf{E} = \left[e_1,e_2,e_3\right]^{\mathrm{T}}$ is the supply voltages vector, $\mathbf{I} = \left[i_1,i_2,i_3\right]^{\mathrm{T}}$ is the corresponding currents vector, $\mathbf{V}_C = \left[v_A,v_B\right]^{\mathrm{T}} = \left[v_{C1},v_{C0}\right]^{\mathrm{T}}$ is the vector of the voltages at points A and B, $\mathbf{V}_D = \left[v_{D1},\dots,v_{D6}\right]^{\mathrm{T}}$ is the diodes voltages vector. The matrices $\mathbf{T}_1$, $\mathbf{T}_2$, $\mathbf{C}$ and $\mathbf{D}$ are defined as follows:

$$\mathbf{T}_1 = \begin{bmatrix} 1 & 0 & 0 & -1 & 0 & 0 \\ 0 & 1 & 0 & 0 & -1 & 0 \\ 0 & 0 & 1 & 0 & 0 & -1 \end{bmatrix}, \mathbf{T}_2 = \begin{bmatrix} 1 & 1 & 1 & 0 & 0 & 0 \\ 0 & 0 & 0 & -1 & -1 & -1 \end{bmatrix},$$

$$\mathbf{C} = \begin{bmatrix} C_1 & 0 \\ 0 & C_0 \end{bmatrix}, \quad \mathbf{D} = \mathrm{diag}\left[g_1(v_{D1}),\dots,g_6(v_{D6})\right]$$

where $g_i(v_{Di})$ are the nonlinear conductance function describing the diode electrical behavior. The IGBT inverters are controlled by using the PWM technique with a switching frequency sufficiently high to consider true the following relation, see (Espinoza *et al.*, 2001):

$$v_{Li}(t) = u_i\, v_B(t) + (1 - u_i)\, v_A(t) \qquad (1)$$

where $u_i \in [0,1]$. If $u_i = 0 \Rightarrow v_{Li}(t) = v_A(t)$, if $u_i = 1 \Rightarrow v_{Li}(t) = v_B(t)$. The transformation matrix $\mathbf{U}$ realizes the inverter ideal function (1):

$$\mathbf{U} = \begin{bmatrix} 1-u_1 & 1-u_2 & \dots & 1-u_m \\ u_1 & u_2 & \dots & u_m \end{bmatrix}$$

Note that matrix $\mathbf{U}$ is a function of the control vector $\mathbf{u} = \left[u_1,\dots,u_m\right]^{\mathrm{T}}$. The lamps-loads, roughly approximated as linear elements, can be described by using the following resistance and inductance matrices:

$$\mathbf{R} = \begin{bmatrix} R_{L1} & 0 & \dots & 0 \\ 0 & R_{L2} & \dots & 0 \\ \vdots & \vdots & \ddots & \vdots \\ 0 & 0 & \dots & R_{Lm} \end{bmatrix}, \mathbf{L} = \begin{bmatrix} L_{L1} & 0 & \dots & 0 \\ 0 & L_{L2} & \dots & 0 \\ \vdots & \vdots & \ddots & \vdots \\ 0 & 0 & \dots & L_{Lm} \end{bmatrix}$$

The vectors $\mathbf{V}_L = \left[v_{L1},v_{L2},\dots,v_{Lm}\right]^{\mathrm{T}}$ and $\mathbf{I}_L = \left[i_{L1},i_{L2},\dots,i_{Lm}\right]^{\mathrm{T}}$ represent the load voltages and load currents.

4. PROPOSED CONTROL LAWS

4.1 Sinusoidal load voltages

To cope with requirement (1) of Section 2.1, the following load voltages have to be imposed:

$$v_{Li}(t) = V_{Li}\sin(\omega\, t + \varphi_i) \qquad (2)$$

where V_{Li} are the voltage amplitudes, φ_i are the phase angles, $\omega = 2\,\pi\, f$ and $f = 50$ Hz is the frequency of the sinusoidal signals. To impose these voltages, two different control laws can be used.

1) The *first control law* is the following:

$$u_i(t) = \frac{1}{2} + \frac{V_{Li}}{220\sqrt{2}}\sin(\omega\, t + \varphi_i) \qquad (3)$$

The value $\frac{1}{2}$ is necessary for the IGBT polarization. This is the simplest "feed-forward" control law which tries to satisfy requirement (2) of Section 2.1 without using any sensor. Unfortunately, it can not impose perfect sinusoidal voltages on the loads because the two intermediate voltages $v_A(t)$ and $v_B(t)$ are time-varying and unknown.

2) The *second control law* can be easily obtained by inverting relations (1)-(2), in fact:

$$u_i(t) = \frac{v_A(t) - V_{Li}\sin(\omega\, t + \varphi_i)}{v_A(t) - v_B(t)} \qquad (4)$$

This control law ensures perfect sinusoidal voltages on the loads, but it can be used only if the two voltages $v_A(t)$ and $v_B(t)$ are known. The phase angles φ_i are free parameters that will be used for the minimization of the neutral current i_N, see Section 4.3.

Simulation results showing the effectiveness of the two proposed control laws (3) and (4), are reported in Fig. 5. The parameters used in simulation are: $m = 3$, $|e_i| = 220\sqrt{2}$ V, $r_d = 0.1\ \Omega$, $C_0 = C_1 = 2$ mF, $R_{L1} = 7.1\ \Omega$, $R_{L2} = 12.5\ \Omega$, $R_{L3} = 10\ \Omega$, $L_{L1} = 14.08$ mH, $L_{L2} = 24.64$ mH, $L_{L3} = 19.71$ mH, $\varphi_1 = 0$, $\varphi_2 = 120^o$ and $\varphi_3 = 240^o$. The simulation has been divided in

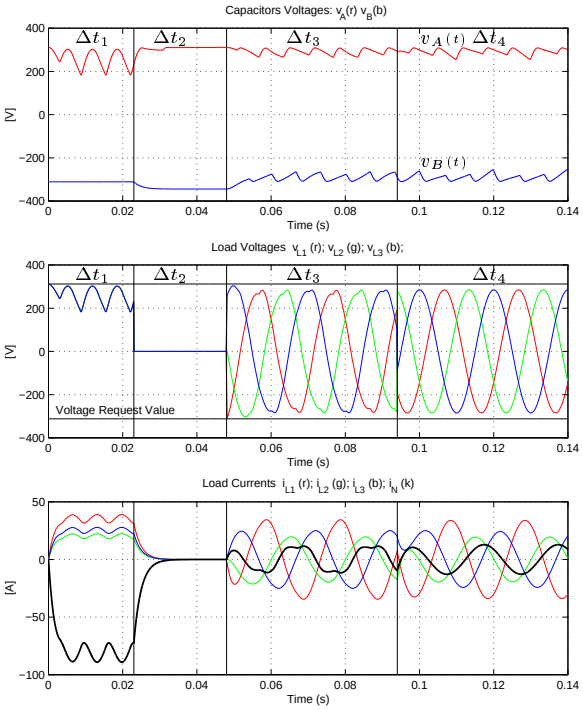

Fig. 5. Time behavior of voltages and currents on the load.

four time intervals Δt_1, Δt_2, Δt_3 and Δt_4. In each time interval a different control law has been used. In the first time interval Δt_1 the control $\mathbf{u}$=$\mathbf{0}$ has been used, obtaining the load voltages $v_{Li}(t) = v_A(t)$. The load currents $\mathbf{I}_L$ have different amplitudes because the impedances of the loads are different. In Fig. 5 the neutral current i_N is also reported in solid thick line. In the second time interval Δt_2 the control law $u_i(t) = \frac{v_A(t)}{v_A(t)-v_B(t)}$ has been applied. In steady state condition it ensures zero load voltages $\mathbf{V}_L$=$\mathbf{0}$ and zero load currents $\mathbf{I}_L$=$\mathbf{0}$. In the third time interval Δt_3 the feed-forward control law (3) has been applied. From the figure, it is evident that the ripple on the voltages $v_A(t)$ and $v_B(t)$ is partially transferred to the load voltages, and so the load currents are not perfectly sinusoidal. In the last time interval Δt_4 the proposed control law (4) has been used. From Fig. 5 it is evident that now the voltages $\mathbf{V}_L$ and the currents $\mathbf{I}_L$ are perfectly sinusoidal.

4.2 Load voltages amplitude

From Fig. 5 it is easy to see that the load peak voltages do not reach the voltage $\pm 220\sqrt{2}$ required by the control requirement (2) of Section 2.1. In fact, due to the presence of losses in the rectifier and in the inverters, the required load voltage 220 Vrms cannot be reached if the amplitude of the input voltage is 220 Vrms. To increase the maximum value of the load voltages $\mathbf{V}_L$ is necessary to increase the voltages at the points A and B. A boost circuit for charging the capacitors C_1 and C_0 at the desired values is a possible solution,

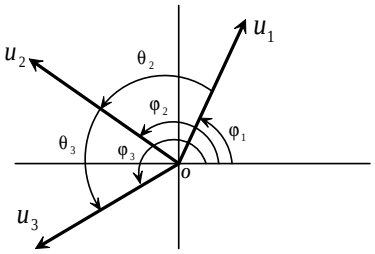

Fig. 6. Phase angles φ_i and relative angles θ_i.

but it is very expensive. A cheaper and simpler solution is the insertion of an autotransformer at the input of the rectifier. By properly choosing the transformation ratio τ of the autotransformer one can ensure load voltages $\mathbf{V}_L$ of 220 Vrms even in the presence of a fluctuation of $\pm 10\%$ on the amplitudes of the supply voltages $\mathbf{E}$.

4.3 Minimization of the neutral current

The neutral current i_N is given by relation:

$$i_N = -\sum_{j=1}^{m} i_{Lj} \tag{5}$$

that is, the current i_N is zero only when the sinusoidal load currents i_{Lj} are balanced. If in control law (4) one chooses $\varphi_1 = 0$, $\varphi_2 = 120^o$ and $\varphi_3 = 240^o$, the load voltages $\mathbf{V}_L$ are balanced and the neutral current i_N is zero only if the three load impedances are equal. See for example the time internal Δt_4 shown in Fig. 5: in this case the current i_N is not zero because the load impedances used in simulation are not balanced.

4.3.1. Neutral current minimization: ideal case

The neutral current i_N can be minimized by properly acting on the phases φ_i of the control inputs u_i given in (4). In fact, the control inputs u_i induce sinusoidal load voltages $\mathbf{V}_L$ characterized by the same phase angles φ_i, see eq. (2). If linear loads are considered, the load currents i_{Li} are sinusoidal too, but with phase angles depending on the load impedances. So, with a proper choice of the phase angles φ_i, one can minimize the neutral current i_N, see (5). In steady state condition, the amplitude I_N of the sinusoidal current i_N can be expressed as follows:

$$I_N = \left| -\sum_{i=1}^{m} \frac{V_{Li}\, e^{j\,\varphi_i}}{R_{Li} + j\omega\, L_{Li}} \right| \tag{6}$$

For the I_N minimization is not important the actual values of the angles φ_i, but the relative angles $\theta_2 = \varphi_2 - \varphi_1$ and $\theta_3 = \varphi_3 - \varphi_1$, see Fig. 6 for the case $m = 3$. These two angles θ_2 and θ_3 can be considered as the new control inputs for the minimization problem. In the ideal case, if the impedance parameters R_{Li} and L_{Li} are known, one can easily verify that the neutral current i_N is zero when:

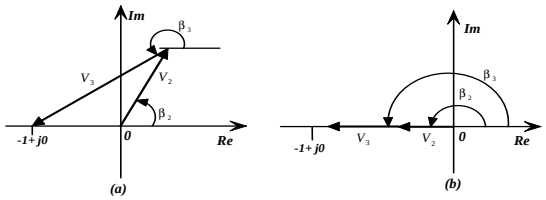

Fig. 7. Graphical representation of relation (9).

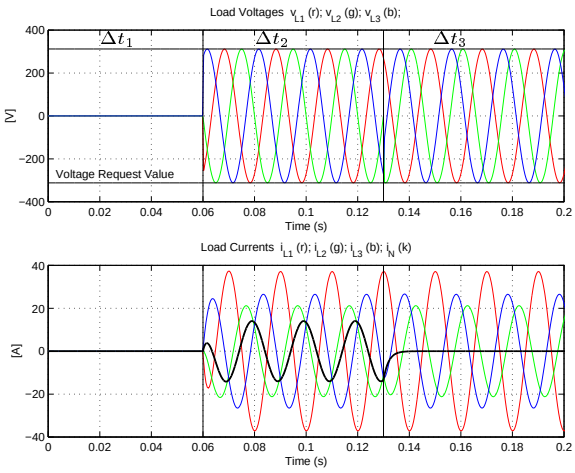

Fig. 8. Control of the neutral current i_N: load voltages and load currents.

$$\theta_2 = \alpha_2 - \alpha_1 \pm \beta_2; \quad \theta_3 = \alpha_3 - \alpha_1 \pm \beta_3 \qquad (7)$$

where $\alpha_i = \arctan(\omega\, L_{Li}/R_{Li})$, $i = \{1,2,3\}$ and

$$\beta_2 = \arccos\left(\frac{V_3^2 - 1 - V_2^2}{2\,V_2}\right), \quad \beta_3 = -\arccos\left(\frac{V_2^2 - 1 - V_3^2}{2\,V_3}\right)$$
$$V_2 = \frac{V_{L2}}{V_{L1}}\frac{\sqrt{R_{L1}^2 + \omega^2\, L_{L1}^2}}{\sqrt{R_{L2}^2 + \omega^2\, L_{L2}^2}}, \quad V_3 = \frac{V_{L3}}{V_{L1}}\frac{\sqrt{R_{L1}^2 + \omega^2\, L_{L1}^2}}{\sqrt{R_{L3}^2 + \omega^2\, L_{L3}^2}} \qquad (8)$$

The two solutions (7) satisfy the following complex expression, see Fig. 7 (a),

$$V_2\, e^{j\beta_2} + V_3\, e^{j\beta_3} + 1 = 0 \qquad (9)$$

which is verified only if:

$$V_2 + V_3 \geq 1, \qquad |V_3 - V_2| \leq 1 \qquad (10)$$

When these inequalities are not satisfied, the amplitude I_N cannot be zero. In this case the minimum value of I_N is obtained if in (7) the following parameters are used, see Fig. 7 (b):

$$\begin{cases} \beta_2 = \pi,\ \beta_3 = \pi & \text{if } V_2 + V_3 < 1 \\ \beta_2 = \pi,\ \beta_3 = 0 & \text{if } (V_2 + V_3 \geq 1) \wedge (V_3 - V_2 \geq 1) \\ \beta_2 = 0,\ \beta_3 = \pi & \text{if } (V_2 + V_3 \geq 1) \wedge (V_2 - V_3 \geq 1) \end{cases} \qquad (11)$$

Simulation results referring to case (7) are shown in Fig. 8. The simulation parameters are the same used in Fig. 5 with $|e_i| = 195\sqrt{2}$ V and with the presence of an autotransformer with $\tau = 1.2$. In the first time interval Δt_1 the control signals $u_i(t) = \frac{v_A(t)}{v_A(t) - v_B(t)}$ ensure $\mathbf{V}_L = \mathbf{0}$. The control law (4) has been used in the second time interval Δt_2: the amplitudes and the phase angles used in this case are: $|v_{Li}| = 220\sqrt{2}$, $\theta_2 = 120^0$ and $\theta_3 = 240^0$. The neutral current i_N is not zero

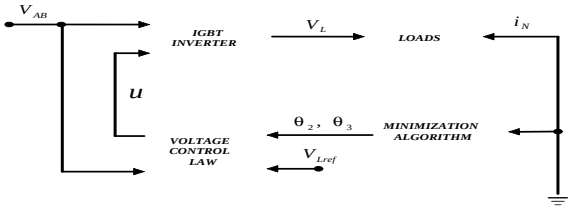

Fig. 9. Feedback control scheme for the minimization of the neutral current i_N.

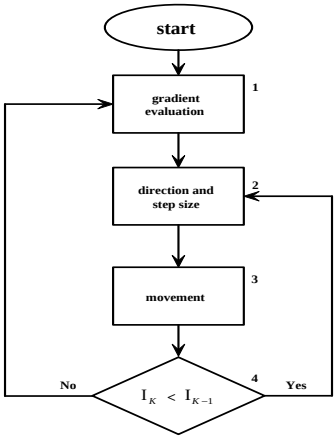

Fig. 10. Flow chart of the minimization algorithm.

because the load currents are not balanced. In the third time interval Δt_3 the control law (4) has been used with phase angles satisfying the relation (7) and (8): $\theta_2 = 136^o$ and $\theta_3 = 214^o$. In this case, the neutral current i_N rapidly converges to zero.

4.3.2. Minimization current algorithm The relations (7) can be used only if the loads parameters are known. Unfortunately, the resistances R_{Li} and the inductances L_{Li} are typically unknown. A possibile solution of this problem is the use of the feedback control scheme shown in Fig. 9: a current sensor measures the current i_N and a properly designed control algorithm modifies the phase angles θ_2 and θ_3 trying to minimize the amplitude I_N of the sinusoidal neutral current i_N. The flow chart of the minimization algorithm is reported in Fig. 10. The algorithm acts as follows: it measures the current amplitude I_N; it evaluates the gradient $\overrightarrow{\text{grad}}(I_N) = \left[\frac{\partial I_N}{\partial \theta_2}, \frac{\partial I_N}{\partial \theta_3}\right]^T$ by adding little phase increments $\Delta\theta_2$, $\Delta\theta_3$ to phase angles θ_2 and θ_3; the gradient vector $\overrightarrow{\text{grad}}(I_N)$ is the maximum growing direction of the function $I_N = f(\theta_2, \theta_3)$ and therefore the current i_N decreases if the new phase angles θ_2 and θ_3 are chosen with increments opposed to the gradient direction. This dynamic behavior can be described by the following discrete equations:

$$\begin{cases} (\theta_2)_{k+1} = (\theta_2)_k - \delta_k \left(\dfrac{\partial I_N}{\partial \theta_2}\right)_k \\ (\theta_3)_{k+1} = (\theta_3)_k - \delta_k \left(\dfrac{\partial I_N}{\partial \theta_3}\right)_k \end{cases}$$

where δ_k is the step amplitude that can be chosen constant or function of the current amplitude I_N. The proposed algorithm has been designed to be always active: in this way, if the load impedances change, the algorithm is able to track the movement of the new minimum point. This algorithm can also be used for nonlinear loads (for example neon lamps) if, in steady state conditions, the function $I_N(\theta_2, \theta_3)$ has only one minimum point. A mesh representation of the

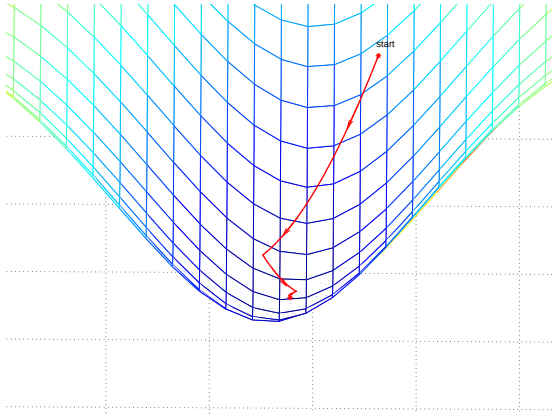

Fig. 11. Mesh plot of function $I_N = f(\theta_2, \theta_3)$.

function $I_N = f(\theta_2, \theta_3)$ obtained from (6) is shown in Fig. 11. The loads parameters used in this case are: R_{L1}=7.1 Ω, R_{L2}=30 Ω, R_{L3}=40 Ω, L_{L1}=14.1 mH, L_{L2}=24.7 mH and L_{L3}=19.8. The initial conditions are: $\theta_2 = 120^o$, $\theta_3 = 240^o$ and $I_N = 28.7$ A. In Fig. 11 it is also reported the trajectory obtained by using the proposed minimization algorithm. The contour plot of function

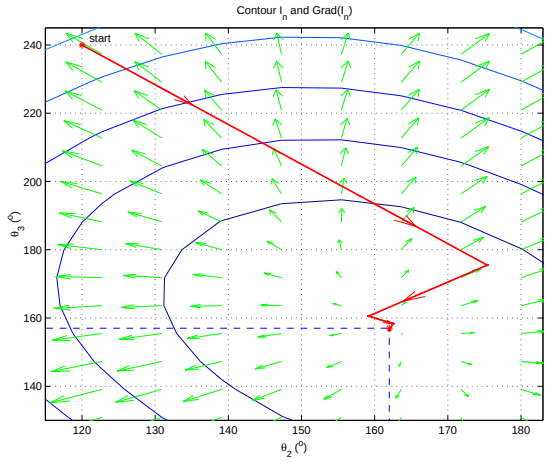

Fig. 12. Contour plot of function $I_N = f(\theta_2, \theta_3)$.

$I_N = f(\theta_2, \theta_3)$ together with the obtained trajectory are shown in Fig. 12. The algorithm slowly reaches the point $\theta_2 = 162.5^o$, $\theta_3 = 159^o$ and $I_N = 19.3$ A, which corresponds to the minimum point that can also be obtained by using the relations (7), (8) and (11). In this case the amplitude I_N of the return current i_N does not reach the zero value because the load parameters used in simulation do not satisfy relation (10). In fact, in this case we have $V_2 = 0.27$, $V_3 = 0.20$, $\beta_2 = \pi$ and $\beta_3 = \pi$: it is the case shown in Fig. 7 (b).

5. CONCLUSIONS

In this paper the problem of modelling and simulating a lighting system has been considered. All the components of the system have been modelled by using the Power-Oriented Graphs technique. Simple control laws for controlling the load voltages $\mathbf{V}_L$ and for minimizing the neutral current i_N have been also proposed. The performance of the controlled model has been tested through simulation experiments.

6. ACKNOWLEDGEMENT

The authors want to thank Prof. A. Massarini and Ing. F. Burani for their technical support and their comments during the preparation of this work.

REFERENCES

Espinoza J. R., G. Joos, J. I. Guzmàn, L. A. Morán and R. P. Burgos (2001). "Selective Harmonic Elimination and Current/Voltage Control in Current/Voltage - Source Topologies: A Unified Approach", *IEEE Transactions on Industrial Electronics*, Vol 48, *N*. 1.

Hui S.Y.R., L. M. Lee, H. S.-H. Chung and Y.K. Ho (2001). An Electric Ballast with Wide Dimming Range, High PF, and Low EMI. *IEEE Transactions on Power Electronics*, Vol 16, *N*. 4.

Hur N., J. Jung, and K. Nam (2001). A Fast Dynamic DC-Link Power-Balancing Scheme for a PWM Converter- Inverter System. *IEEE Transactions on Industrial Electronics*, Vol 48, *N*. 4.

Karnopp, D.C., Rosemberg R.C. (1975). *System dynamics: a unified approach*, Wiley, N.Y.

Nerone L.R. (2001). Novel Self-Oscillating ClassE Ballast for Compact Fluorescent Lamps. *IEEE Transactions on Power Electronics*, Vol 16, N^2.

Park H.-W., S.-J Park, J.-G Park, and C.-U Kim (2001). A Novel High-Performance Voltage Regulator for Single Phase AC Sources. *IEEE Transactions on Industrial Electronics*, Vol 48, *N*. 3.

Paynter, H.M. (1961). *Analysis and Design of Engineering Systems*, MIT-press, Camb., MA.

Zanasi R. (1991.) Power Oriented Modelling of Dynamical System for Simulation. *IMACS Symp. on Modelling and Control of Technological System*, Lille, France.

Zanasi R. (1994). Dynamics of a *n*-links Manipulator by Using Power-Oriented Graph. *SYROCO '94*, Capri, Italy.